


Origin of Blue Luminescence in Mg-Doped GaN

Sanjay Nayak,^{1,*} Mukul Gupta,² Umesh V. Waghmare,³ and S.M. Shivaprasad¹

¹*Chemistry and Physics of Materials Unit, Jawaharlal Nehru Centre for Advanced Scientific Research (JNCASR), Bangalore 560064, India*

²*UGC-DAE Consortium for Scientific Research, University Campus, Khandwa Road, Indore 452001, India*

³*Theoretical Sciences Unit, Jawaharlal Nehru Centre for Advanced Scientific Research (JNCASR), Bangalore 560064, India and Sheikh Saqr Laboratory, Jawaharlal Nehru Centre for Advanced Scientific Research (JNCASR), Bangalore 560064, India*

 (Received 22 August 2017; revised manuscript received 8 October 2018; published 14 January 2019)

We uncover the origin of the blue luminescence (BL) peak in a Mg-doped GaN thin film using a combination of experimental x-ray absorption near-edge spectroscopy (XANES), first-principles calculations based on density functional theory (DFT), and full multiple scattering (FMS) theoretical analysis of various possible defect complexes and their XANES signatures. We demonstrate that a defect complex composed of Mg substituted at a Ga site (Mg_{Ga}) and Mg at an interstitial site (Mg_i) is primarily responsible for the observed BL by a donor–acceptor pair transition (DAP) associated with a deep donor state in the gap. It correlates with a higher (lower) oxidation state of N (Ga) in heavily Mg-doped GaN than in its pristine structure, evident in our experiments as well as calculations. Physical and chemical mechanisms identified here point out a route to achieving efficient *p*-type GaN, which has been one of the major limiting factors in obtaining highly efficient GaN-based optoelectronic devices.

DOI: [10.1103/PhysRevApplied.11.014027](https://doi.org/10.1103/PhysRevApplied.11.014027)

I. INTRODUCTION

Gallium nitride (GaN) is a wide-band-gap semiconductor ($E_g = 3.51$ eV at 2 K) extensively used for solid-state lighting [1], high power and high frequency devices [2], and lasers [3]. It is essential to have both *n*- and *p*-type semiconducting GaN to develop GaN/(In, Ga)N quantum-well-(QW)-based optoelectronic devices. Despite intensive research in the last few decades, some material issues related to GaN remain open to be resolved [4], e.g., the origin of unintentional *n*-doped behavior of native GaN. Although GaN-based light emitting diode (LEDs) have already been commercialized, their optimal performance has yet to be realized, partly because of the difficulties in the efficient incorporation of *p*-type carriers in the host. To date, magnesium (Mg) is the only *p*-type dopant to have been successfully employed in the fabrication of *p*-GaN. However, a high ionization energy of Mg in GaN [5] (approximately 200 meV) requires a relatively high concentration of Mg in the fabrication of efficient *p*-GaN. Secondly, higher Mg incorporation in GaN leads to the formation of point defects and/or defect complexes and consequent self-compensation in Mg-doped GaN [6].

The incorporation of Mg in GaN results in characteristic luminescence peaks depending on the dopant concentration. Mg doping of $<10^{19}$ atoms cm^{-3} in GaN

results in luminescence peaks at 3.270 and 3.466 eV (at $T = 2$ K) [7], while at high concentration ($>10^{19}$ atoms cm^{-3}), a dominant PL peak appears in the range of 2.70–2.95 eV, known as blue luminescence (BL) [8], the origin of which has been debated in the literature extensively in the past decade [9–15]. Recent density functional theory (DFT)-based calculations suggest that the emergence of BL is due to different ionization energies of nitrogen vacancies (V_{N}) [16] and of hole localization at neighboring N atoms [17]. This result, however, fails to explain the absence of BL from the samples with lower Mg concentrations. Moreover, no direct experimental evidence has yet been reported corroborating these mechanisms.

Here, we report a photoluminescence (PL) and XANES spectroscopic study of undoped and Mg-doped GaN thin films. We analyze the experimentally acquired XANES spectra by correlating them with results of first-principles simulations of various defect complexes and decipher the characteristic features. Further, we use the electronic structure of the relevant defect complexes obtained from DFT-based simulations to identify the luminescence centers in Mg-doped GaN.

II. METHODS

A. Experimental details

The Mg-doped GaN thin films are synthesized in the nanowall network (NwN) geometry on a (0001) plane of

*sanjaynayak@jncasr.ac.in

sapphire (α -Al₂O₃) by a plasma-assisted molecular-beam-epitaxy (PAMBE) system (SVTA-USA). The gallium (Ga) effusion cell is maintained at 1030 °C. A constant nitrogen flow rate of 8 sccm (standard cubic centimeters per minute), substrate temperature of 630 °C, plasma forward power of 375 W, and growth duration of 4 h are employed in the growth of all the films. Mg and Ga fluxes are obtained by measuring the beam equivalent pressures (BEP), which are varied by controlling the temperature of the respective K cells. Optical emission of the films is characterized by photoluminescence spectroscopy (PL, Horiba Jobin Yvon) using a Xenon lamp (short arc lamp, UXL-450S-O, USHIO Inc.) source with 325-nm excitation. XANES spectra of these samples are recorded in the total-electronic-yield (TEY) mode at the SXAS beam line (BL-01) of the Indus-2 Synchrotron Source at the Raja Ramanna Centre for Advanced Technology (RRCAT), Indore, India [18]. The optical system of the BL-01 of the Indus-2 Synchrotron Source beamline contains a toroidal mirror to focus the beam on the sample surface (vertically as well as horizontally). The slit widths before the monochromator and sample are 1 and 0.1 mm, respectively. The energy resolution in the acquired spectra is better than 0.2 eV. The details of the experimental setup for XANES measurements are given in Ref. [18]. A typical data reduction procedure (background removal and normalization) of the XANES spectra is performed using the Athena software package [19].

Details of the other growth process and structural properties can be found elsewhere [20]. We present an analysis of three samples of GaN films here: one pristine sample *A* (labelled as Mg:Ga = 0.0000) and two doped (namely, *B* and *C*), where the sample *C* is grown with higher Mg flux (Mg:Ga = 0.1102) than that used for *B* (Mg:Ga = 0.0393).

B. Simulation details

In the simulation of XANES spectra, we carry out first-principles DFT calculations using a combination of many codes. First, we use the Siesta code [21] to obtain the optimized atomic structure of defect configurations, where a local density approximation (LDA) of Ceperley and Alder [22] with Perdew and Zunger [23] parametrization of the exchange and correlation energy functional is used. Integrations over the Brillouin zone of *w*-GaN are sampled on a Γ -centered $5 \times 5 \times 3$ uniform mesh of \mathbf{k} -points in a unit cell of reciprocal space [24]. We relax positions of all atoms to minimize energy using a conjugate-gradients algorithm until the forces on each atom are less than 0.04 eV/Å. Our optimized lattice parameters of the pristine GaN are $a = 3.173$ Å and $c = 5.163$ Å, which are in good agreement with the experimental values [25] ($a = 3.186$ Å and $c = 5.189$ Å). In simulation of GaN with defect(s), we consider a $4 \times 4 \times 2$ supercell (128 atoms).

The formation energy of defects (for a neutral state) in the bulk is calculated using the Zhang-Northrup scheme [26], given by

$$E_f = E_{\text{tot}}(\text{defect}) - E_{\text{tot}}(\text{pristine}) + \sum n_i \mu_i,$$

where $E_{\text{tot}}(\text{defect})$ and $E_{\text{tot}}(\text{pristine})$ are the total energies of supercells containing a defect and the reference pristine structure, respectively. n_i and μ_i represent the number of atoms added or removed [if atom(s) are added, it will take a positive sign, whereas if atom(s) are removed, it will take a negative sign] and the chemical potential of the i^{th} species, respectively. In this work, we calculate the defect formation energy under N-rich conditions. Under N-rich conditions, μ_{N} is the energy of a N atom [obtained from the total energy $E_{\text{tot}}(\text{N}_2)$ of a N₂ molecule, i.e., $\mu_{\text{N}} = \frac{1}{2}E_{\text{tot}}(\text{N}_2)$]. The chemical potential of Ga is calculated using the assumption of thermodynamic equilibrium, i.e., $\mu_{\text{Ga}} + \mu_{\text{N}} = E_{\text{GaN}}[\text{bulk}]$, where $E_{\text{GaN}}[\text{bulk}]$ is the total energy of one formula unit. We use the chemical potential of Mg (μ_{Mg}) as the energy of a single Mg atom in the hcp phase [$\mu_{\text{Mg}} = \frac{1}{2}E_{\text{tot}}(\text{Mg}_{\text{hcp}})$], noting that the primitive unit cell of the hcp structure contains two atoms.

From the relaxed atomic structure obtained from Siesta calculations, we construct clusters in calculations to determine the *ab initio* XANES spectra with FEFF9.05 code [27], where the Hedin-Lundqvist exchange potential with an imaginary part of 0.2 eV is used and an exchange core hole is treated according to the final state rule in the simulation of *K*-edges. We calculate the atomic potential for a cluster of 128 atoms with a radius of 8 Å and determined the full multiple scattering XANES spectra by increasing the cluster radius to 12.5 Å around the absorber.

To determine the electronic structure and gap states of the relevant defect configurations, we use the HSE06 [28] hybrid functional as implemented in vasp code [29]. In these calculations, we use optimized lattice parameters and a relaxed atomic structure obtained from Siesta calculations, where the local density approximation (LDA) of Ceperley and Alder is used for the exchange and correlation energy functional. The reference valence electronic configurations of Ga, N, and Mg are considered as $3d^{10}4s^24p^1$, $2s^22p^3$, and $3s^23p^0$, respectively. We use an energy cutoff of 500 eV to truncate the plane wave basis. The electronic energy spectrum at the Γ point is calculated by using the Heyd-Scuseria-Ernzerhof (HSE) hybrid functional, where the mixing parameter for the Hartree-Fock exchange potential is set at 25%. The screening parameter in HSE calculations is fixed at 0.2.

III. EXPERIMENTAL RESULTS

We choose GaN NwN as the host in the present work because of the superior optical properties of the film; e.g.,

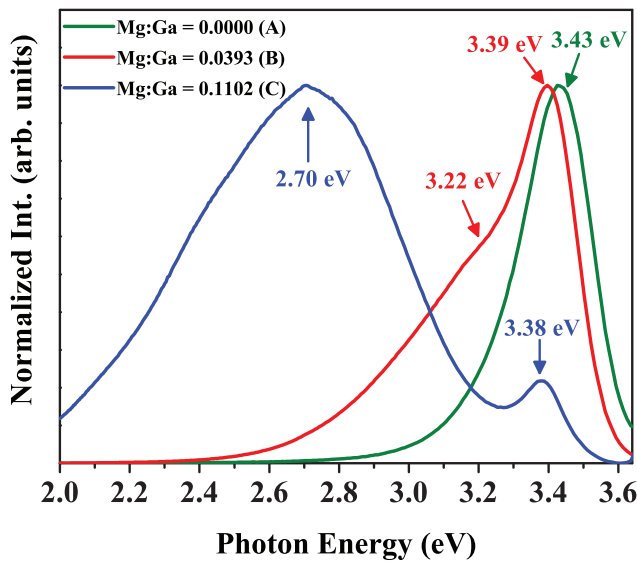


FIG. 1. Normalized room temperature photoluminescence (PL) spectra of samples *A*, *B*, and *C*.

they do not show any other luminescence peak(s) except near band-edge emission (NBE). A thorough structural characterization of the samples is carried out using HR-XRD and Raman spectroscopy and the results have been published elsewhere [20]. Though the morphology of GaN NwN samples is different, their crystal structure, lattice parameters, optical band gap, native *n*-type character of as-grown undoped samples, and epitaxial relation with the substrate are similar to the flat epilayers grown using metal-organic chemical vapor deposition (MOCVD). The microstructure of the film consists of a dense network of tapering GaN nanowalls that are single crystalline with a wurtzite structure, showing a band gap of approximately 3.4 eV. Since our samples are grown using the PAMBE system, concentrations of impurities such as hydrogen, carbon, and other organometallic species in these samples are negligible, in contrast to the relatively higher density of defects in MOCVD grown films.

We find that all three samples considered here are single crystalline and have wurtzite crystal structure and are *c*-oriented with no sign of any cubic phase [30] in the grown samples (see Sec. II of Supplemental Material). In the PL spectra obtained at RT (see Fig. 1), sample *A* shows only one dominant luminescence peak centered at 3.43 eV, assigned to the NBE emission of GaN, whereas sample *B* exhibits two distinct peaks, centered at 3.39 and 3.22 eV, respectively. While the peak centered at 3.39 eV is assigned to the NBE of GaN, the peak centered at 3.22 eV is assigned to an electron-acceptor (e-A) or DAP transition in Mg-doped GaN [7]. PL spectra of sample *C* show two distinct luminescence features, and they are identified as the NBE at 3.38 eV and the intense BL peak centered at 2.70 eV, respectively.

To understand the origin of different luminescence peaks as observed in the PL spectra of samples, it is useful to study the electronic structure of all samples using XANES because of its effectiveness in determining the element or site-specific properties [31]. To this end, we probe the N *K*-edge and Ga *L*_{2,3}-edge of the three samples using XANES [see Figs. 2(a) and 2(b)]. For the N *K*-edge, five distinct features (P1–P5) are seen clearly, which are consistent with earlier observations [32]. We consider the absorption edge as the location of the first significant peak in the first derivative of absorbance [$\mu(E)$] with respect to energy [i.e., $d\mu(E)/dE$] [33] [see Fig. 2(c)]. It is seen that the N *K*-edges (P1') of samples *A* and *B* do not show any significant changes in their absorption threshold, whereas that of sample *C* shows a shift of approximately 0.7 eV toward higher energy relative to that of *A*, suggesting a small increase in the oxidation state of N atoms in sample *C*. Along with a change in the absorption edge, we also observe a clear distortion of the peak P1. The peak intensity of P1 of sample *C* is higher and more pronounced than that of samples *A* and *B* [see Fig. 2(a)]. This increase in the peak intensity of P1 with higher Mg incorporation is consistent with an earlier

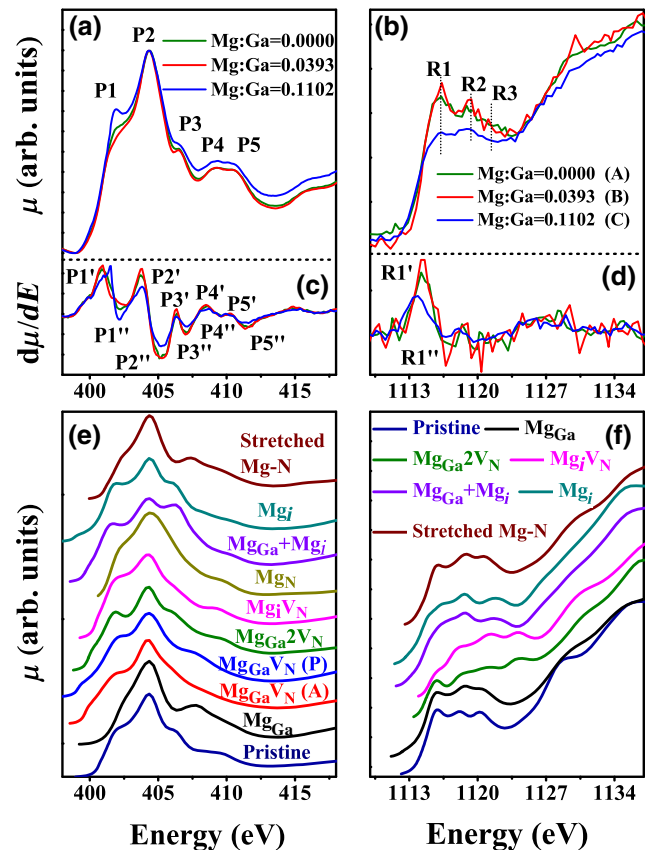


FIG. 2. XANES spectra of normalized N *K*-edges (a) and Ga *L*_{2,3} edges (b), respectively. The first derivative plot of N *K*-edge and Ga *L*_{2,3} are shown in (c) and (d), respectively. Simulated XANES spectra N *K*-edge and Ga *L*₃-edge for various defect configurations are presented in (e) and (f), respectively.

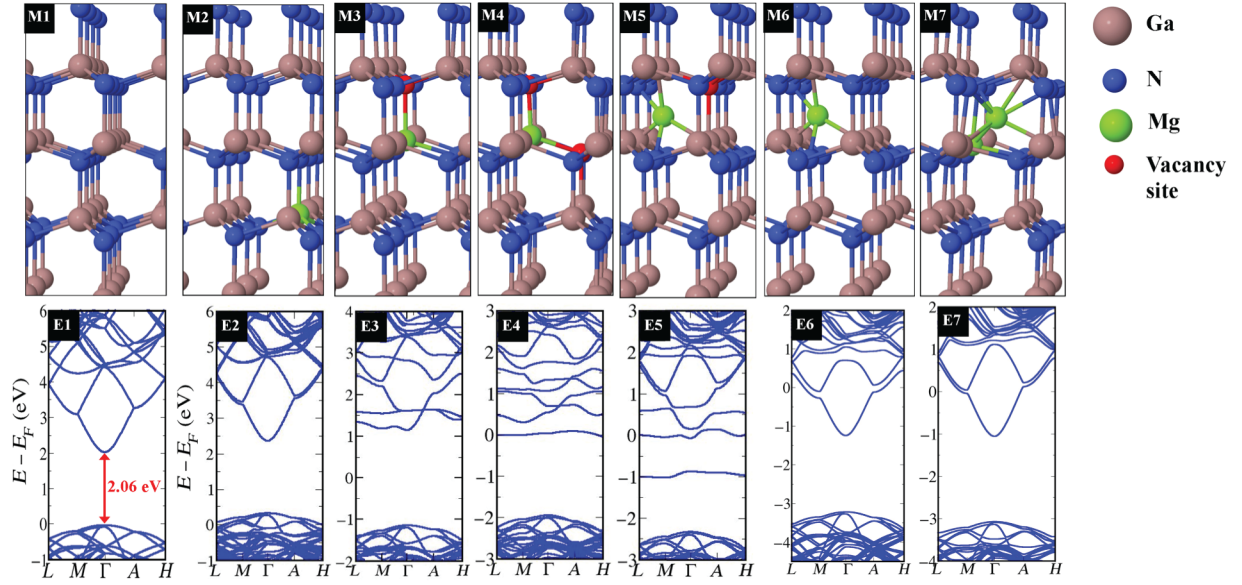


FIG. 3. M1–M7 show ball-and-stick models of different configurations used in DFT and multiple scattering theory calculations: (M1) pristine w-GaN, (M2) Mg substituted at a Ga site (Mg_{Ga}), (M3) a complex of Mg substituted at a Ga site and a nitrogen vacancy ($Mg_{Ga} - V_N$), (M4) a complex of Mg substituted at a Ga site and two nitrogen vacancies ($Mg_{Ga} - 2V_N$), (M5) a complex of Mg at an interstitial site and a nitrogen vacancy ($Mg_i - V_N$), (M6) Mg at an interstitial site (Mg_i), and (M7) a complex of Mg substituted at a Ga site and Mg at an interstitial site ($Mg_{Ga} + Mg_i$). E1–E7 show the electronic structure of different defect configurations shown as M1–M7, respectively, which are obtained from Siesta (DFTLDA). The Fermi level is set at 0 eV.

report [34]. Increase in the intensity of the feature P1 may arise from the localized states that form due to higher Mg incorporation in the film.

Recorded $L_{2,3}$ edge spectra of Ga atoms are presented in Fig. 2(b), with the first derivative of the L_3 -edge in Fig. 2(d). Similar to the N K -edge, we do not observe any changes in the absorption threshold of samples *A* and *B*. However, we observe a small redshift (approximately 0.80 eV) for sample *C*, indicating reduction in the oxidation states of Ga atoms. The two distinct features R1 and R2 are seen clearly in all three samples. For samples *A* and *B*, the intensity of R1 is higher than that of R2, whereas for the sample *C*, the intensity of R2 is higher than that of R1, with a flat absorption profile near the L_3 -edge.

IV. THEORETICAL ANALYSIS AND DISCUSSIONS

To uncover the origin of observed changes and features in experimental XANES spectra as a function of the Mg-doping concentration, we obtain *ab initio* XANES spectra. We focus on three possible mechanisms, which are widely speculated to be the origins of the BL in the literature: (i) nitrogen vacancy complexes, (ii) the configuration with hole localization, and (iii) Mg interstitial defect complexes [ball-and-stick models are shown in Fig. 3 (M1–M7)]. Before studying the relevance of vacancy complexes to XANES spectra, we benchmark the simulation parameters

with a careful analysis of the pristine GaN (see Sec. I of the Supplemental Material). Clearly, there is good agreement between our theory and experiment, as well as with results reported earlier [35].

The simulated N K - and Ga L_3 -edges in XANES spectra of the substitutional Mg at Ga site (Mg_{Ga}) are shown in Figs. 2(e) and 2(f), respectively. We find that peak P1, obtained from the simulation of the configuration with the (Mg_{Ga}) defect, is not very prominent and has a lower intensity relative to the pristine GaN. This reduction in the intensity of P1 is consistent with the behavior shown by sample *B*. We infer that no other defect complexes are present notably in sample *B* and the luminescence peak centered at 3.22 eV is due to the recombination of an e-A pair. A Mulliken population analysis from the results of Siesta calculations suggests a small increase in the oxidation states of both first nearest-neighbor (NN) N (approximately $0.05|e|$) atoms and first NN Ga (approximately $0.016|e|$) atoms that coordinate the site of the Mg substituent in Mg-doped GaN relative to that of undoped GaN (see Table I). Despite this small increase in oxidation states of N and Ga atoms seen in our simulations, we do not observe a significant change in the absorption edges of sample *B*, due to significantly lower incorporation of Mg in the host.

Further, we simulate several defect configurations: (i) complexes of Mg_{Ga} with a single N vacancy ($Mg_{Ga} - V_N$), with two N vacancies ($Mg_{Ga} - 2V_N$), and with Mg at an

TABLE I. Neutral defect formation energy of different defect complexes in N-rich conditions. The Mulliken charges of the first NN of the defect complex are given with reference to pristine GaN. The negative (positive) sign in the Mulliken charge indicates an increase (decrease) in the oxidation state.

Defect configuration	Formation energy (eV)	Mulliken charge in $ e $	
		NN N	NN Ga
Mg_{Ga}	1.20	-0.050	-0.016
$\text{Mg}_{\text{Ga}}V_{\text{N}}$	0.51	-0.015	+0.152
$\text{Mg}_{\text{Ga}}2V_{\text{N}}$	4.91	-0.046	+0.181
Mg_iV_{N}	8.47	-0.056	+0.242
Mg_{N}	9.78	-0.064	+0.074
$\text{Mg}_{\text{Ga}} + \text{Mg}_i$	-0.17	-0.061	+0.055
Mg_i	4.80	-0.015	+0.068

interstitial site ($\text{Mg}_{\text{Ga}} + \text{Mg}_i$); (ii) a complex of Mg at an interstitial site with a nitrogen vacancy ($\text{Mg}_i - V_{\text{N}}$); (iii) Mg at a nitrogen site (antisite defect) (Mg_{N}); and (iv) Mg at an interstitial site (Mg_i). The characteristic signatures of these configurations in the XANES spectra are shown in Figs. 2(e) and 2(f). In the configurations of $\text{Mg}_{\text{Ga}} - V_{\text{N}}$, we consider N vacancies in the axial and basal planes of the w-GaN, as the four Ga—N bonds in GaN_4 tetrahedra are not the same. We find that the former configuration is energetically more favorable and do not observe any significant change in the characteristics of XANES spectra with respect to pristine GaN. Thus, the increase in the peak P1 of sample C cannot be attributed to the formation of a $\text{Mg}_{\text{Ga}} - V_{\text{N}}$ complex.

A comparison between the experimental and simulated results for XANES spectra clearly suggests that the possible causes for the enhanced intensity of the P1 feature in the N K -edge of sample C can be $\text{Mg}_{\text{Ga}} - 2V_{\text{N}}$, $\text{Mg}_i - V_{\text{N}}$, $\text{Mg}_{\text{Ga}} + \text{Mg}_i$, or Mg_i . Mulliken charges of N atoms near these defect complexes due to the formation of defect complexes are listed in Table I along with the formation energies. Clearly, the oxidation states of N (Ga) atoms increase (decrease) slightly in these defect configurations. Thus, a clear conclusion on the determination of dominant defect(s) could not be reached from the Mulliken population analysis alone. Further, our estimates of the formation energies of these defect complexes obtained using the Zhang-Northrup scheme [26] (see Table I) reveal that the defect configuration $\text{Mg}_{\text{Ga}} + \text{Mg}_i$ has the lowest formation energy and is probably the most preferable defect complex that should form in Mg-doped GaN. Recently, Miceli *et al.* [36] and Reshchikov *et al.* [37] predicted from hybrid-functional-based DFT calculations that Mg interstitial is the energetically preferable defect in Mg-doped GaN, which was neglected earlier due to overestimation of its formation energy with a semilocal functional [38,39], which is consistently evident in the results of our calculations here (see Table I). Simulated L_3 edge spectra of the

configurations $\text{Mg}_{\text{Ga}} + \text{Mg}_i$ and Mg_i show [see Fig. 2(f)] that the peak R2 has a higher intensity than R1, as observed experimentally only for sample C. Thus, we propose that the observed increase in the intensity of P1 of sample C is due to the increase in the unoccupied donor states, originating from the formation of the defect complex $\text{Mg}_{\text{Ga}} + \text{Mg}_i$ and/or Mg_i . Further, the shift in the absorption threshold of N K -edges of sample C in comparison to sample A is due to the reduction in the Mulliken charges (oxidation states) of N atoms of the MgN_4 tetrahedra. We find the relaxed atomic structure of GaN containing the $\text{Mg}_{\text{Ga}} + \text{Mg}_i$ defect complex shows an elongation of the axial Mg—N bond by 14%, while one Mg—N bond in the basal plane contracts by 2.5% and the other two Mg—N bonds stretch by 5.4% relative to the Ga—N bonds of pristine GaN.

To connect with the prediction of van de Walle *et al.* [17], we simulate the XANES spectra of N K - and Ga L_3 -edges by stretching the Mg—N bond to a value 15% higher than the Ga—N bond, while allowing other atoms to relax [see Figs. 2(e) and 2(f)]. We do not see any significant change in the N K -edge with respect to pristine GaN. Thus, the distortion of peak P1 in Fig. 2(a) cannot be attributed to the longer Mg—N bond.

As DFTLDA typically underestimates the band gap [the band gap of GaN calculated with siesta is 2.06 eV; see Fig. 3(E1)], much lower than its experimental value of 3.51 eV, we use hybrid-HSE06-functional-based calculations to determine the energy levels of the defect states in the electronic structure using Vasp code (see Fig. 4). In these simulations with a $4 \times 4 \times 2$ supercell, we use only the Γ -point in sampling the Brillouin zone integrations. Our estimate of the band gap of pristine GaN is 3.36 eV, reasonably close to the experimentally observed band gap of 3.51 eV at $T = 2$ K and 3.43 eV observed at RT in this study. For the configuration Mg_{Ga} , we find a shallow acceptor state (approximately 0.22 eV above the VBM), which has a predominant N-2p orbital character. Configurations with ($\text{Mg}_{\text{Ga}} + \text{Mg}_i$) and Mg_i exhibit deep donor states in the electronic gap at approximately 3.14 and 3.07 eV above VBM. Thus, the transition from the deep donor state to the shallow acceptor state occurs at (3.14–0.22) approximately 2.92 eV, very close to the emission peak of BL (2.7 eV) observed in sample C (see Fig. 4). We note that the concentration of Mg in our simulations of Mg-doped GaN is higher than that used in the experiment and yields this small difference. Although in the past a similar mechanism (the transition between deep donor and shallow acceptor) on the origin of BL has been proposed, its atomistic origin is not yet clear [11,40]. An alternative mechanism claimed by Lyons *et al.* [17], where BL is a result of transitions of electrons from the conduction band to the deep and localized Mg_{Ga} acceptor level, fails to explain large shifts in the BL peak with the increase in excitation intensity and the absence of the BL peak in lightly doped samples. The work of Buckeridge *et al.* [16], which suggests that the BL

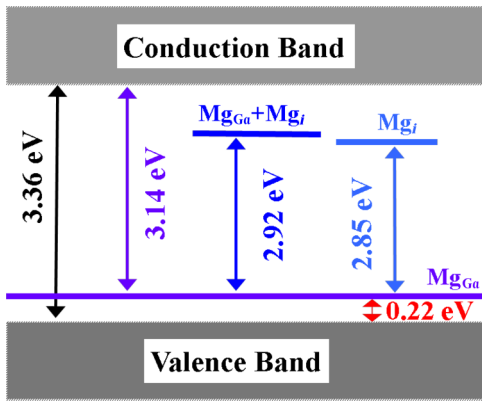


FIG. 4. A schematic of the electronic structure of heavily Mg-doped GaN obtained with hybrid-HSE06-functional-based calculations (at Γ point).

is due to the formation of isolated V_N , is in contradiction with other reports [16,41] and also suffers from accuracy issues in the calculations [42,43]. Recently, Wahl *et al.* [44] studied the site occupancy of Mg in GaN by implanting radioactive Mg in GaN and found a notable amount of Mg in interstitial sites, while the majority of them occupied substitutional Ga sites. As mentioned earlier, some reports [36,37] suggest that the formation energy of Mg occupying an interstitial site is less in *p*-type GaN. Thus, Mg may prefer to be at the interstitial sites in the films during the epitaxial growth process.

As the epitaxial growth temperature of GaN is reasonably high (630 °C in the present work), mobility of Mg adatoms is high during growth. When Mg at an interstitial site diffuses close to a Ga vacancy site in the process, it takes up the same and becomes substitutional Mg at the Ga site in GaN [44]. In the films grown under the low Mg flux, the occurrence of Mg_{Ga} is expected to be dominant, resulting in the formation of a shallow acceptor state in the electronic gap and the associated 3.22-eV peak in the luminescence spectra. In contrast, during the epitaxial growth with higher Mg flux, the number of available Ga vacancy sites are not abundant enough for diffusing Mg_i to get converted to Mg_{Ga} . Instead, Mg_i adatoms will pair up with other suitable defects due to their relatively low formation energy and form defect complexes such as $Mg_{Ga} + Mg_i$, which create a deep donor state in the electronic gap. Our work shows that these defect complexes are responsible for the BL emission arising from the deep donor to shallow acceptor state transitions. Further, the mechanism proposed in this study on the origin of BL clearly explains the the large shift of the peak position with the increase in excitation intensity and absence of BL in lightly doped samples. Based on our analysis, we propose that the synthesis of *p*-type GaN with a high hole concentration can be achieved by imposing Ga-poor growth conditions rather than Ga-rich conditions.

V. SUMMARY

In summary, we uncover the origin of observed BL in Mg-doped GaN through a combination of experiments and theoretical analysis of Mg incorporated at different concentrations in GaN thin films. With clear evidence in PL and XANES of heavily Mg-incorporated GaN films, we show that the observed BL originates from defect complexes formed of interstitial Mg (Mg_i) and substitutional Mg (Mg_{Ga}). The BL is associated with a transition from the deep donor state in the electronic gap to the shallow acceptor state. Our experiments reveal a slightly higher oxidation state of N and lower oxidation state of Ga in heavily Mg-incorporated GaN than those in pristine GaN that are supported well by our first-principles calculations.

ACKNOWLEDGMENTS

S.N. acknowledges JNCASR for financial support. The authors gratefully acknowledge JNCASR; UGC-DAE CSR; and RRCAT, Indore, for providing facilities. U.V.W. acknowledges support from a JC Bose National Fellowship and a Sheikh Saqr fellowship.

- [1] Russell D. Dupuis, Michael R. Krames, and Senior Member, History, development, and applications of high-brightness visible light-emitting diodes, *J. Light. Technol.* **26**, 1154 (2008).
- [2] S. T. Sheppard, K. Doverspike, W. L. Pribble, S. T. Allen, J. W. Palmour, L. T. Kehias, and T. J. Jenkins, High-power microwave GaN/AlGaIn HEMT's on semi-insulating silicon carbide substrates, *IEEE Electron Device Lett.* **20**, 161 (1999).
- [3] Tien Chang Lu, Tsung Ting Kao, Shin Wei Chen, Chih Chiang Kao, Hao Chung Kuo, and Shing Chung Wang, CW lasing of current injection blue GaN-based vertical cavity surface emitting lasers, *Appl. Phys. Lett.* **92**, 141102 (2008).
- [4] Chris G. Van De Walle and Jörg Neugebauer, First-principles calculations for defects and impurities: Applications to III-nitrides, *J. Appl. Phys.* **95**, 3851 (2004).
- [5] M. Zhang, P. Bhattacharya, W. Guo, and A. Banerjee, Mg doping of GaN grown by plasma-assisted molecular beam epitaxy under nitrogen-rich conditions, *Appl. Phys. Lett.* **96**, 132103 (2010).
- [6] I. P. Smorchkova, E. Haus, B. Heying, P. Kozodoy, P. Fini, J. P. Ibbetson, S. Keller, S. P. DenBaars, J. S. Speck, and U. K. Mishra, Mg doping of GaN layers grown by plasma-assisted molecular-beam epitaxy, *Appl. Phys. Lett.* **76**, 718 (2000).
- [7] B. Monemar, P. P. Paskov, G. Pozina, C. Hemmingsson, J. P. Bergman, S. Khromov, V. N. Izyumskaya, V. Avrutin, X. Li, H. Morkoc, H. Amano, M. Iwaya, and I. Akasaki, Properties of the main Mg-related acceptors in GaN from optical and structural studies, *J. Appl. Phys.* **115**, 053507 (2014).

- [8] M. A. Reshchikov and H. Morkoç, Luminescence from defects in GaN, *Phys. B Condens. Matter* **376**, 428 (2006).
- [9] Ryohei Nonoda, Kanako Shojiki, Tomoyuki Tanikawa, Shigeyuki Kuboya, Ryuji Katayama, and Takashi Matsuoka, Effects of Mg/Ga and V/III source ratios on hole concentration of N-polar (000-1) p-type GaN grown by metalorganic vapor phase epitaxy, *Jpn. J. Appl. Phys.* **55**, 05FE01 (2016).
- [10] L. Eckey, U. von Gfug, J. Holst, A. Hoffmann, A. Kaschner, H. Siegle, C. Thomsen, B. Schineller, K. Heime, M. Heuken, O. Schön, and R. Beccard, Photoluminescence and Raman study of compensation effects in Mg-doped GaN epilayers, *J. Appl. Phys.* **84**, 5828 (1998).
- [11] M. Reshchikov, G.-C. Yi, and B. Wessels, Behavior of 2.8- and 3.2-eV photoluminescence bands in Mg-doped GaN at different temperatures and excitation densities, *Phys. Rev. B* **59**, 13176 (1999).
- [12] Eunsoon Oh, Hyeongsoo Park, and Yongjo Park, Excitation density dependence of photoluminescence in GaN:Mg, *Appl. Phys. Lett.* **72**, 70 (1998).
- [13] U. Kaufmann, P. Schlotter, H. Obloh, K. Köhler, and M. Maier, Hole conductivity and compensation in epitaxial GaN:Mg layers, *Phys. Rev. B* **62**, 10867 (2000).
- [14] S. Hautakangas, V. Ranki, I. Makkonen, M. J. Puska, K. Saarinen, L. Liskay, D. Seghier, H. P. Gislason, J. A. Freitas, R. L. Henry, X. Xu, and D. C. Look, Gallium and nitrogen vacancies in GaN: Impurity decoration effects, *Phys. B Condens. Matter* **376**, 424 (2006).
- [15] S. Hautakangas, K. Saarinen, L. Liskay, J. Freitas, and R. Henry, Role of open volume defects in Mg-doped GaN films studied by positron annihilation spectroscopy, *Phys. Rev. B* **72**, 165303 (2005).
- [16] J. Buckeridge, C. R. A. Catlow, D. O. Scanlon, T. W. Keal, P. Sherwood, M. Miskufova, A. Walsh, S. M. Woodley, and A. A. Sokol, Determination of the Nitrogen Vacancy as a Shallow Compensating Center in GaN Doped with Divalent Metals, *Phys. Rev. Lett.* **114**, 016405 (2015).
- [17] John L. Lyons, Anderson Janotti, and Chris G. Van De Walle, Shallow versus Deep Nature of Mg Acceptors in Nitride Semiconductors, *Phys. Rev. Lett.* **108**, 156403 (2012).
- [18] D. M. Phase, Mukul Gupta, S. Potdar, L. Behera, R. Sah, Ajay Gupta, Chitra Murlu, D. Bhattacharyya, and S. C. Gadkari, in *AIP Conference Proceedings* (AIP, 2014), Vol. 1591, p. 685.
- [19] Bruce Ravel and M. Newville, Athena, artemis, hephaestus: Data analysis for x-ray absorption spectroscopy using ifeffit, *J. Synchrotron Radiat.* **12**, 537 (2005).
- [20] S. K. Nayak, M. Gupta, and S. M. Shivaprasad, Structural, optical and electronic properties of Mg incorporated GaN Nanowall Network, *RSC Adv.* **7**, 25998 (2017).
- [21] Jose M. Soler, Emilio Artacho, Julian D. Gale, Alberto Garcia, Javier Junquera, Pablo Ordejon, and Daniel Sanchez-Portal, The SIESTA method for ab initio order-N materials simulation, *J. Phys. Condens. Matter* **14**, 2745 (2001).
- [22] D. M. Ceperley and B. J. Alder, Ground State of the Electron Gas by a Stochastic Method, *Phys. Rev. Lett.* **45**, 566 (1980).
- [23] J. P. Perdew and Alex Zunger, Self-interaction correction to density-functional approximations for many-electron systems, *Phys. Rev. B* **23**, 5048 (1981).
- [24] Hendrik J. Monkhorst and James D. Pack, Special points for Brillouin-zone integrations, *Phys. Rev. B* **13**, 5188 (1976).
- [25] M. Leszczynski, I. Grzegory, H. Teisseyre, T. Suski, M. Bockowski, J. Jun, J. M. Baranowski, S. Porowski, and J. Domagala, The microstructure of gallium nitride monocystals grown at high pressure, *J. Cryst. Growth* **169**, 235 (1996).
- [26] S. B. Zhang and John E. Northrup, Chemical Potential Dependence of Defect Formation Energies in GaAs: Application to Ga Self-diffusion, *Phys. Rev. Lett.* **67**, 2339 (1991).
- [27] John J. Rehr, Joshua J. Kas, Fernando D. Vila, Micah P. Prange, and Kevin Jorissen, Parameter-free calculations of X-ray spectra with FEFF9, *Phys. Chem. Chem. Phys.* **12**, 5503 (2010).
- [28] Jochen Heyd, Gustavo E. Scuseria, and Matthias Ernzerhof, Hybrid functionals based on a screened coulomb potential, *J. Chem. Phys.* **118**, 8207 (2003).
- [29] G. Kresse and J. Furthmüller, Efficient iterative schemes for ab initio total-energy calculations using a plane-wave basis set, *Phys. Rev. B* **54**, 11169 (1996).
- [30] O. Zsebök, J. V. Thordson, J. R. Gunnarsson, Q. X. Zhao, L. Ilver, and T. G. Andersson, The effect of the first GaN monolayer on the nitridation damage of molecular beam epitaxy grown GaN on GaAs (001), *J. Appl. Phys.* **89**, 3662 (2001).
- [31] Heiko Wende, Recent advances in x-ray absorption spectroscopy, *Reports Prog. Phys.* **67**, 2105 (2004).
- [32] W. R. L. Lambrecht, S. N. Rashkeev, B. Segall, K. LawniczakJablonska, T. Suski, E. M. Gullikson, J. H. Underwood, R. C. C. Perera, J. C. Rife, I. Grzegory, S. Porowski, and D. K. Wickenden, X-ray absorption, glancing-angle reflectivity, and theoretical study of the N K- and Ga M(2,3)-edge spectra in GaN, *Phys. Rev. B* **55**, 2612 (1997).
- [33] E. M. Bittar, C. Adriano, T. M. Garitezi, P. F. S. Rosa, L. Mendonça-Ferreira, F. Garcia, G. D. M. Azevedo, P. G. Pagliuso, and E. Granado, Co-substitution Effects on the Fe Valence in the BaFe₂As₂ Superconducting Compound: A Study of Hard X-ray Absorption Spectroscopy, *Phys. Rev. Lett.* **107**, 267402 (2011).
- [34] Y. C. Pan, S. F. Wang, W. H. Lee, W. C. Lin, C. I. Chiang, H. Chang, H. H. Hsieh, J. M. Chen, D. S. Lin, M. C. Lee, W. K. Chen, and W. H. Chen, Structure study of GaN:Mg films by X-ray absorption near-edge structure spectroscopy, *Solid State Commun.* **117**, 577 (2001).
- [35] M. S. Moreno, K. Jorissen, and J. J. Rehr, Practical aspects of electron energy-loss spectroscopy (EELS) calculations using FEFF8, *Micron* **38**, 1 (2007).
- [36] Giacomo Miceli and Alfredo Pasquarello, Self-compensation due to point defects in Mg-doped GaN, *Phys. Rev. B* **93**, 165207 (2016).
- [37] Michael A. Reshchikov, D. O. Demchenko, J. D. McNamara, S. Fernández-Garrido, and R. Calarco, Green luminescence in Mg-doped GaN, *Phys. Rev. B* **90**, 035207 (2014).

- [38] Chris G. Van de Walle, Jörg Neugebauer, Catherine Stampfl, M. D. McCluskey, and N. M. Johnson, Defects and defect reactions in semiconductor nitrides, *ACTA Phys. Pol. A* **96**, 613 (1999).
- [39] J. Neugebauer and C. G. Van de Walle, in *Proceedings of the Materials Research Symposia of Gallium Nitride and Related Materials*, edited by R. D. Dupuis, J. A. Edmond, F. A. Ponce, and S. Nakamura (Materials Research Society, Pittsburgh, Pennsylvania, 1995), p. 645.
- [40] H. Teisseyre, T. Suski, P. Perlin, I. Grzegory, M. Leszczynski, M. Bockowski, S. Porowski, J. A. Freitas, R. L. Henry, A. E. Wickenden, and D. D. Koleske, Different character of the donor-acceptor pair-related 3.27 eV band and blue photoluminescence in Mg-doped GaN. Hydrostatic pressure studies, *Phys. Rev. B* **62**, 10151 (2000).
- [41] Qimin Yan, Anderson Janotti, Matthias Scheffler, and Chris G. Van de Walle, Role of nitrogen vacancies in the luminescence of Mg-doped GaN, *Appl. Phys. Lett.* **100**, 142110 (2012).
- [42] D. O. Demchenko and M. A. Reshchikov, Comment on “Determination of the Nitrogen Vacancy as a Shallow Compensating Center in GaN Doped with Divalent Metals”, *Phys. Rev. Lett.* **115**, 029701 (2015).
- [43] J. L. Lyons, A. Alkauskas, A. Janotti, and C. G. Van de Walle, First-principles theory of acceptors in nitride semiconductors, *Phys. Status Solidi B* **252**, 900 (2015).
- [44] U. Wahl, L. M. Amorim, V. Augustyns, A. Costa, E. David-Bosne, T. A. L. Lima, G. Lippertz, J. G. Correia, M. R. da Silva, M. J. Kappers, K. Temst, A. Vantomme, and L. M. C. Pereira, Lattice Location of Mg in GaN: A Fresh Look at Doping Limitations, *Phys. Rev. Lett.* **118**, 095501 (2017).